Generation and characterization of terahertz pulse trains from biased, large-aperture photoconductors

C. W. Siders, J. L. W. Siders, and A. J. Taylor

Materials Science and Technology Division, Los Alamos National Laboratory, Los Alamos, New Mexico 87545

S.-G. Park, M. R. Melloch, and A. M. Weiner

School of Electrical and Computer Engineering, Purdue University, West Lafayette, Indiana 47907

Received September 28, 1998

The saturation properties of terahertz emission from biased, large-aperture photoconductors excited by trains of amplified femtosecond optical pulses are presented. A direct comparison is made of the multiple-pulse saturation properties of terahertz emission from semi-insulating GaAs and low-temperature-grown GaAs emitters with different carrier lifetimes. When the carrier lifetime is less than or comparable with the interpulse spacing, a significant enhancement of the narrow-band terahertz output is observed. The enhancement is not observed for emitters with long carrier lifetimes, consistent with the results of a previously derived saturation theory [Opt. Lett. **18,** 1340 (1993)]. © 1999 Optical Society of America

OCIS codes: 320.7160, 320.7080, 320.7100, 320.7130.

The development of new sources of terahertz (THz) radiation optimized for particular scientific or technological applications is being pursued by a number of groups of researchers. Broadband THz radiation (0.1–2 THz) is often produced by generation of an ultrafast current surge in a photoconductive switch excited by an above-bandgap femtosecond (fs) optical pulse.[1] For many applications, such as radar and microwave communications, far-infrared nonlinear optics, and coherent control of materials,[2] generation of THz pulse trains,[3] which often results in narrow-band radiation, is desired. Generation of narrow-band THz radiation has been demonstrated by use of a train of optical pulses, derived either through the interference of a pair of highly chirped optical pulses[4] or through fs pulse shaping,[5] incident upon a biased photoconductor. In the latter case, complex THz pulse trains can be generated by manipulation of the input optical pulse trains. Finally, pulse trains of THz radiation have been generated by optical rectification of femtosecond optical pulse trains in electro-optic materials.[6,7]

To scale to higher-energy THz pulse trains, the use of amplified optical pulses incident upon biased, large-aperture photoconductive emitters is necessary. Several groups of researchers have studied the physical mechanisms that limit the radiated THz power for such emitters under single-pulse excitation.[1,8] Liu *et al.*[5] studied the saturation properties of the THz emission from low-temperature-grown GaAs (LT-GaAs) dipole emitters excited with oscillator-level pulse trains and demonstrated that by using a pulse sequence for excitation one can avoid saturation effects and enhance the narrow-band THz output. We present here a direct comparison of the saturation properties of the THz radiation from semi-insulating GaAs (SI-GaAs) and several LT-GaAs large-aperture emitters excited by trains of amplified femtosecond pulses. Our studies demonstrate avoidance of saturation through multiple-pulse excitation, and a strong enhancement of the peak power spectral density, for large-aperture emitters with carrier lifetimes shorter than the interpulse spacing. Our results also confirm that the saturation recovery time depends on the photocurrent lifetime, consistent with the results of a previously derived saturation theory.[8]

The experimental setup is described as follows: An amplified Ti:sapphire laser system produces 130-fs, 0.7-mJ pulses at 800 nm with a repetition rate of 1 kHz. Roughly 90% of this beam is input into a novel hyper-Michelson interferometer,[7] which is used to produce a pulse train of 2–8 equal-amplitude pulses separated by 3.3 ps, corresponding to a repetition rate of 300 GHz. The optical pulse train is lightly focused to a 4-mm-diameter spot and is incident upon a 5-mm-gap photoconductive emitter biased at 3 kV/cm. The photoconductors studied consist of a 1-mm-thick SI-GaAs sample and three samples each of which has a 2.8-μm-thick LT-GaAs layer grown upon a 0.6-mm-thick SI-GaAs substrate. The LT-GaAs layers were grown at 280 °C by molecular beam epitaxy and subsequently annealed for 30 s at 575, 600, and 625 °C.[9] For the SI-GaAs sample the carrier lifetime is >100 ps, whereas for the LT-GaAs samples the lifetimes are all <10 ps. The 2.8-μm thickness is chosen for the LT-GaAs layer to prevent carriers generated in the SI-GaAs substrate from contributing to the THz signal. Electo-optic detection of the emitted far-field THz waveform with a 1-mm thick ZnTe crystal is implemented.

Figure 1 reveals THz waveforms measured from SI-GaAs and LT-GaAs (annealed at 600 °C) emitters. For the SI-GaAs emitter the waveform that results from single-pulse excitation is shown as curve (a) of Fig. 1; waveforms that result from eight-pulse excitation in the low- (20-μJ/cm^2) and high- (500-μJ/cm^2) fluence regimes are shown as curves (b) and (c). For multiple-pulse excitation we use the term "fluence" to refer to the total fluence integrated over all

0146-9592/99/040241-03$15.00/0

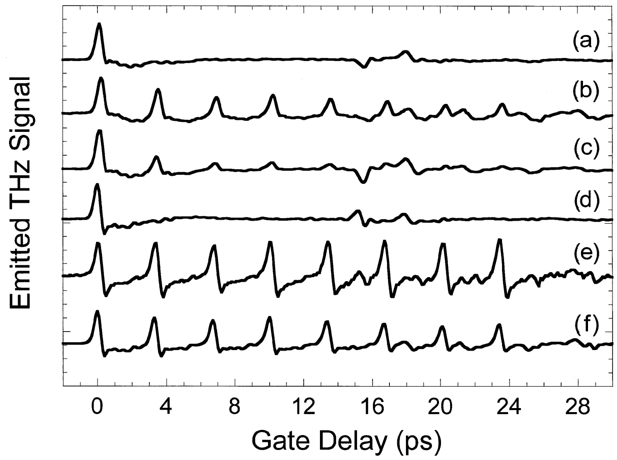

Fig. 1. THz waveforms measured from (a)–(c) SI-GaAs and (d)–(f) LT-GaAs (annealed at 600 °C) emitters for (a), (d) single-pulse excitation and for eight-pulse excitation in the (b), (e) low-, 20-$\mu J/cm^2$, and (c), (f) high-, 500-$\mu J/cm^2$, fluence regimes. The waveforms are individually normalized.

excitation pulses. For the LT-GaAs emitter, waveforms measured under the same conditions as for the SI-GaAs emitter are shown in curves (d)–(f). There is clearly a striking difference in the fluence dependence of the waveforms emitted from SI-GaAs and LT-GaAs emitters. At low fluences in both materials the eight-pulse THz waveform approximates a linear combination of eight single-pulse waveforms. However, at high fluences the waveform emitted from SI-GaAs is distorted, exhibiting a strong initial pulse and subsequent pulses decreasing in amplitude, whereas the waveform from the LT-GaAs emitter is relatively undistorted.

The difference in behavior between SI-GaAs and LT-GaAs is caused by the different carrier lifetimes in the two materials. In SI-GaAs the carrier lifetime is >100 ps, and therefore the photocurrent excited by the first pulse in the train does not recover before the arrival of the next pulse. Because it is this current that limits the THz output, each subsequent pulse is diminished in amplitude as a result of the previous pulses' contribution to the photocurrent. For the LT-GaAs emitter the carrier lifetime at the highest fluence studied, as measured by optical pump–THz probe spectroscopy, is 2 ps, thereby allowing the photocurrent that is due to the previous pulse to decay to a small level during the 3.3-ps interpulse separation. Therefore, as preceding pulses in the optical pulse train do not contribute to saturation of the THz output, the resultant THz pulse train for LT-GaAs emitters is undistorted. This saturation behavior is described by the current-surge model of THz emission,[8] which yields a radiated THz field, $E(t)$;

$$E(t) = A\mathrm{d}\sigma(t)/\mathrm{d}t[1 + a\sigma(t)]^{-2}, \qquad (1)$$

where $\sigma(t)$ is the photoinduced conductivity of the emitter and a and A are material- and geometry-dependent constants. In Eq. (1) the factor $[1 + a\sigma(t)]^{-2}$ causes the saturation of the THz output. For SI-GaAs, $\sigma(t)$ increases linearly with each pulse in the train. For LT-GaAs, the contribution to $\sigma(t)$ from previous pulses is negligible because the photoexcited carriers have decayed during the period between pulses; therefore $\sigma(t)$ depends only on the single-pulse fluence.

The saturation behavior exhibited by the LT-GaAs emitter can also result in enhanced narrow-band THz output. With single-pulse excitation at sufficiently high excitation fluences, the THz output saturates at a value determined by the applied bias. If the optical excitation pulse is divided into n equal-amplitude pulses such that each single pulse still yields saturated THz emission and if the spacing between the pulses is large enough that the photoexcited carriers decay between pulses, then the resultant THz output energy will increase by a value approaching n greater than the power produced by a single optical pulse of the same fluence. The peak power spectral density will increase by a factor of n^2 under the same conditions. Such behavior is shown in Fig. 2(a), where the power spectral density at the fundamental frequency of 0.3 THz is plotted versus total optical fluence for a single pulse, a four-pulse train, and an eight-pulse train. At the low-fluence (unsaturated) end the three curves overlap because the THz output in the unsaturated regime depends on the total excitation fluence. At higher fluences, where the single fluence drives the THz emission into saturation, the four-pulse output is enhanced relative to the single-pulse output, and the eight-pulse output is even further enhanced. Indeed, a factor-of-7.5 enhancement in the power spectrum peak is seen at the highest fluences for the eight-pulse case compared with the single pulse case. The enhancement, although it is large, is less than the limit of $n^2 = 64$ because the individual pulses from the train do not fully saturate the emitter and because recovery of the emitter between pulses is incomplete. The same

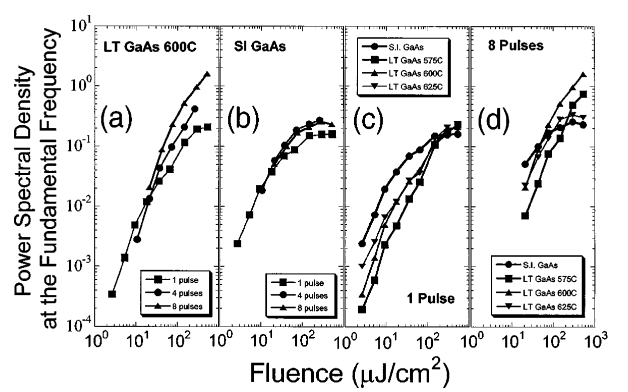

Fig. 2. Power spectral density at the fundamental frequency of 0.3 THz versus total optical fluence for (a) LT-GaAs and (b) SI-GaAs emitters excited by a single pulse, a four-pulse train, and an eight-pulse train. Power spectral density versus total optical fluence and (c) single-pulse excitation and (d) eight-pulse excitation for a SI-GaAs emitter and three LT-GaAs emitters that yield carrier lifetimes ($1/e$) at the highest fluences of <1, 2, and 3 ps following annealing at 575, 600, and 625 °C, respectively. For all curves at low fluences a slope of 2 is observed, indicating that the emission is unsaturated.

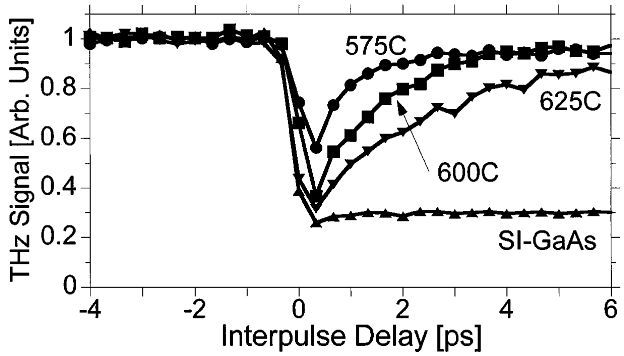

Fig. 3. Peak amplitude of the second emitted THz pulse versus interpulse separation for a SI-GaAs emitter and three LT-GaAs emitters annealed at the three temperatures indicated.

plot, shown in Fig. 2(b) for a SI-GaAs emitter, reveals that the output is independent of the number of pulses. In SI-GaAs, because the photoexcited carriers do not recover between pulses, for a given total optical excitation fluence the saturation behavior of the THz output is independent of the number of pulses.

To further elucidate this saturation behavior we plot the power spectral density versus total optical fluence under single-pulse excitation (Fig. 2(c)] and eight-pulse excitation [Fig. 2(d)] for a SI-GaAs emitter and three LT-GaAs emitters annealed at 575, 600, and 625 °C, resulting in carrier lifetimes ($1/e$) at the highest fluences of <1, 2, and 3 ps, respectively. Under single-pulse excitation [Fig. 2(c)], at high excitation fluences all materials emit the same THz power, determined by the applied bias. At low fluences the THz emission increases with increasing carrier lifetime, because in the unsaturated regime the THz field is proportional to the carrier mobility. The THz saturation behavior under eight-pulse excitation, shown in Fig. 2(d), is similar to the single-pulse data at low fluences; however, at high fluences the enhancement of the THz output is evident in those materials for which the carrier lifetime is significantly shorter than the interpulse spacing. Based on the single-pulse data of Fig. 2(c), further enhancement of the eight-pulse emission from the LT-GaAs emitter (575 °C anneal) with the shortest (<1-ps) lifetime is expected to result in THz power equal to the highest curve (600 °C anneal) at somewhat higher fluences than investigated.

To clarify how this saturation behavior scales with interpulse spacing we vary the separation of two identical optical pulses incident upon an emitter and measure the peak amplitude of second emitted THz pulse.[10] The results are shown in Fig. 3 for an incident per-pulse fluence of 40 $\mu J/cm^2$ (approaching saturation). For SI-GaAs, emission from the second pulse is dramatically reduced relative to that from the first and does not recover as the interpulse separation is increased over the several-picosecond interval studied. For the LT-GaAs emitters the $1/e$ recovery of the THz emission from the second pulse occurs in 0.7 ps for the 575 °C anneal, in 1.3 ps for the 600 °C anneal, and in 3 ps for the 625 °C anneal, consistent with both the lifetime measurements and the multiple-pulse excitation results of Fig. 2.

The data of Figs. 2 and 3 reveal that in terms of designing a multipulse terahertz emitter the 575 °C and 600 °C LT-GaAs materials exhibit distinct application-dependent advantages. The LT-GaAs emitter annealed at 575 °C should yield the best performance at small interpulse separations (<1 ps), as demonstrated with the recovery data; however, the saturation data reveal that a higher optical excitation fluence will be required for output comparable to that of the 600 °C emitter. Indeed, for interpulse spacings greater than 2 ps, the 600 °C LT-GaAs emitter is preferable because it yields higher output at lower fluences. The LT-GaAs emitter annealed at 625 °C would not be so useful because it yielded only slightly more THz output under single-pulse excitation than the 600 °C emitter at low fluences and its recovery time was significantly worse.

In conclusion, we have investigated the saturation properties of THz emission from biased, large-aperture photoconductors excited by trains of amplified fs optical pulses. A direct comparison is made of the multiple-pulse THz emission saturation properties of SI-GaAs and LT-GaAs emitters with different carrier lifetimes. An enhancement of the narrow-band THz output under multiple-pulse excitation is observed only if the carrier lifetime is less than or comparable with the interpulse spacing, consistent with the results of a previously derived saturation theory. These results can be used in the design of optimal emitters to generate high-energy THz pulse trains for applications in communications, nonlinear optics, and coherent control.

A. M. Weiner and S. G. Park acknowledge support from National Science Foundation grants 9404677-PHY and 9722668-PHY. M. R. Melloch acknowledges support from U.S. Air Force Office of Scientific Research grant F49620-96-1-0234A. A. J. Taylor's e-mail address is ttaylor@lanl.gov.

References

1. J. T. Darrow, X.-C. Zhang, D. H. Auston, and J. D. Morse, IEEE J. Quantum Electron. **28,** 2291 (1992).
2. P. G. Huggard, J. A. Cluff, C. J. Shaw, S. R. Andrews, E. H. Linfield, and D. A. Ritchie, Appl. Phys. Lett. **71,** 2647 (1997).
3. N. M. Froberg, B. B. Hu, X.-C. Zhang, and D. H. Auston, Appl. Phys. Lett. **59,** 768 (1991).
4. A. S. Weling, B. B. Hu, N. M. Froberg, and D. H. Auston, Appl. Phys. Lett. **64,** 137 (1994).
5. Y. Liu, S.-G. Park, and A. M. Weiner, IEEE J. Sel. Top. Quantum Electron. **2,** 709 (1996).
6. C. Messner, M. Sailer, H. Kostner, and R. A. Hopfel, Appl. Phys. B **64,** 619 (1997).
7. C. W. Siders, J. L. W. Siders, A. J. Taylor, S.-G. Park, and A. M. Weiner, Appl. Opt. **37,** 5302 (1998).
8. A. J. Taylor, P. K. Benicewicz, and S. M. Young, Opt. Lett. **18,** 1340 (1993).
9. M. R. Melloch, D. D. Nolte, J. C. P. Change, D. B. Janes, and E. S. Harmon, Crit. Rev. Solid State Mater. Sci. **21,** 189 (1996).
10. A. J. Taylor, G. Rodriguez, and D. I. Some, Opt. Lett. **22,** 715 (1997).